

Relation Between Array Excitation Distribution and Radiation Pattern Null Depth

Makoto KIJIMA and Yoshihide YAMADA
 NTT Radio Communication Systems Laboratories
 Yokosuka-shi, Kanagawa-ken, JAPAN

INTRODUCTION

In mobile base station antennas, it has been reported that the narrow radiation pattern nulls are filled in by the effect of the multipath propagation fields [1]. Thus, radiation patterns with and without nulls are considered almost equivalent in the radiation pattern design. Radiation patterns with nulls by array antennas are normal and easily designed, so excitation coefficients along the array elements exhibits flatter distribution. These flatter excitation coefficient distributions have the advantages of ease and accuracy of implementation, considering mutual coupling and manufacturing errors. In past studies on the radiation pattern synthesis, pattern null depth is taken as a measure of design accuracy, and excitation distribution data is given in [2],[3] and [4]. However the relations between excitation coefficient distributions and the design objective radiation pattern null depth are not discussed in detail.

In this paper simple formulas for estimating null depth and excitation distributions are derived by utilizing the Schelkunoff unit circle concept. Calculated results for some design objectives with different sidelobe levels are also shown.

FORMULAS FOR PATTERN NULL DEPTH AND EXCITATION DISTRIBUTION

A typical design objective radiation pattern and a distribution of excitation amplitude are shown in Fig.1(a) and (b), respectively. In Fig.1(a), the null depth is defined as L_{NR} on the right side and L_{NL} on the left side of the radiation pattern. To investigate these characteristics analytically, the Schelkunoff unit circle concept is very effective. Radiation pattern $F(u)$ and excitation coefficients I_n are expressed in a simple form by introducing the complex value W .

$$F(u) = \sum_{n=1}^N I_n W^{n-1} = I_N \prod_{i=1}^{N-1} (W - (1 + \epsilon_i)W_i) \quad (1)$$

Here, $W = \exp(-ju)$, $u = kd \cos \theta$ and $W_i = \exp(-ju_i)$ ($i=1, 2, \dots, N-1$). The roots W_i indicated on the Schelkunoff unit circle and ϵ_i are shown in Fig.2. When $\epsilon_i=0$, all W_i points lie on the unit circle, and the radiation pattern has complete nulls. For $|\epsilon_i| \neq 0$, $(1 + \epsilon_i)W_i$ points are off the unit circle, and $F(u)$ of Eq.1 has no roots. Consequently, pattern nulls are filled in.

From Eq.1, pattern null depth can be derived. The null depth L_{NR} and L_{NL} become nearly equal by using the Schelkunoff method. L_N is then defined as equal to L_{NR} and L_{NL} in Fig.1(a). The bottom level at the k th null point is obtained by inserting u_k into Eq.1. The formula, expressed in dB, becomes

$$G(u_k) \approx 20 \log |\epsilon_k| + \sum_{i=1 (i \neq k)}^{N-1} 10 \log 4(1 + \epsilon_i) \sin^2 \left| \frac{u_i - u_k}{2} \right|. \quad (2)$$

On the other hand, the sidelobe peak level between $\#k$ and $\#(k-1)$ nulls is approximately obtained by inserting $u_p = (u_{k-1} + u_k)/2$ into Eq. 1.

$$G(u_p) \approx \sum_{i=1}^{N-1} 10 \log 4(1 + \epsilon_i) \sin^2 \left| \frac{u_i - u_p}{2} \right| \quad (3)$$

Hence, null depth L_N can be expressed by subtracting Eq.2 from Eq.3

$$L_N \approx -20 \log |\epsilon_k| + C \quad (4)$$

where

$$C = 20 \log \left| \frac{3}{2} \sin \frac{\pi}{2N} \cdot \left\{ \cos \frac{\pi}{2N} \right\}^{N-4} \right|. \quad (5)$$

To derive an expression for C , $u_i \approx 2\pi i / N$ is assumed, considering the W_i positions shown in Fig.2(b). Then, the sine squared terms of Eq.2 and Eq.3 are expressed as $\sin^2 | \pi(i-k)/N |$ and $\sin^2 |$

$n(i-k)/N + \pi/2N$, respectively. Moreover, latter term is approximated to $\sin^2(\pi(i-k)/N) \cdot \cos(\pi/2N)$. Utilizing these approximations for Eq.2 and Eq.3, Eq.5 is obtained. In this expression, it should be noted that the value C depends strongly on N .

Next, the excitation amplitude ratio denoted as R_k in Fig.1(b) is also derived from Eq.1. The k th excitation coefficient I_k is obtained from the coefficient of W_{k-1} in the product expression of Eq.(1).

$$I_k = I_N \sum_{i_1, i_2, \dots, i_{k-1}=1}^{N-1} W_{i_1} W_{i_2} \dots W_{i_{k-1}} \cdot (1 + \varepsilon_{i_1}) \cdot (1 + \varepsilon_{i_2}) \dots (1 + \varepsilon_{i_{k-1}}) \quad (6)$$

The sign of ε_i is changed to approximate symmetry of excitation coefficients around the central element. The values for ε_i are selected as $\varepsilon_1 = -\varepsilon$, $\varepsilon_{N-1} = -\varepsilon$ and $\varepsilon_i = \varepsilon$ ($i=2, \dots, n-2$). Then, terms including both W_1 and W_{n-1} can be written as $(1 + \varepsilon)^{n-k-2}(1 + \varepsilon)^2 \cdot A$. Those terms which include W_1 and W_{n-1} are expressed as $(1 + \varepsilon)^{n-k} C$. The terms which include W_1 or W_{n-1} are expressed as $(1 + \varepsilon)^{n-k-1}(1 + \varepsilon) B$. Using these expressions, Eq.6 would become

$$I_k = I_N (1 + \varepsilon)^{N-k-1} (1 - \varepsilon) \left\{ \frac{1 - \varepsilon}{1 + \varepsilon} A + B + \frac{1 + \varepsilon}{1 - \varepsilon} C \right\} \approx I_N (1 + \varepsilon)^{N-k-2} (A + B + C). \quad (7)$$

Here, $I_N (A + B + C)$ corresponds to the I_k of $\varepsilon=0$, so this value is the excitation coefficient I_{k0} of deep radiation pattern nulls. The important result is that, the ratio of excitation coefficients (I_k / I_{k0}) between filled nulls and those that are not filled is expressed by $(1 + \varepsilon)^{2-k-N}$.

The excitation amplitude ratio between the edge element and the k th element is also derived from Eq.7.

$$R_k \approx (1 + \varepsilon)^{2+k-N} R_{k0} \quad (8)$$

Here, R_k is the excitation amplitude ratio between the edge and the k th element when nulls are filled in. R_{k0} is the excitation amplitude ratio between the edge and center elements when nulls are not filled in. The ratio R_k / R_{k0} can be expressed by only ε , k and N in Eq.8.

NUMERICAL EXAMPLE

First, numerical examples of Eq.4 were obtained, and are shown in Fig.3. The solid lines indicate the calculated data from Eq.4. The data calculated from Eq.1 is also plotted. The sidelobe level near the observed null points is defined as L_s in Fig.3. The data calculated from Eq.4 roughly agrees with that calculated from Eq.1. Judging from the exact data, it should be noted that L_N is not affected by sidelobe level. Curves for L_N depend strongly on N values, and are reduced according to increasing N .

The radiation pattern examples are illustrated in Fig.4. The right side of the pattern is a uniform-excitation pattern and the left side is the Chebychev-excitation pattern with a -40dB sidelobe level. The solid line indicates pattern in $\varepsilon=0$ and the broken line indicates pattern in $\varepsilon=0.1$. They are calculated from Eq.1. All the null depths of $\varepsilon=0.1$ are uniformly 2dB, which roughly agrees with $N=20$ solid line of Fig.3.

The examples of excitation coefficients are illustrated in Fig.5. The solid line indicates excitation coefficients of $\varepsilon=0$, and the broken line $\varepsilon=0.1$. These are calculated from Eq.1. Excitation amplitude distribution can become relatively symmetrical with proper selection of ε_i signs. In this case, the position of the peak excitation amplitude is insensitive to variations in ε_i . Then $k=11$, which is the peak amplitude position, is used in Eq.8. It is thus found that the edge element's excitation amplitude is reduced. The edge element's excitation amplitude becomes 8dB smaller than that in the $\varepsilon=0$ case as shown in Fig.5. Phase changes are rather small.

Calculated amplitude ratios R_k are shown in Fig.6. The solid line indicates the data calculated from Eq.8. The results calculated from Eq.1 are also plotted. The difference between Eq.8 and Eq.1 data is within 3.7dB for $\varepsilon=0.1$ at a sidelobe level of -30dB. R_{k0} corresponds to values in $\varepsilon=0$. R_{k0} decrease as the sidelobe level decreases. On the other hand, R_k / R_{k0} , the ratio between $\varepsilon_i = 0$ and $\varepsilon_i \neq 0$, is determined only by ε_i , and is independent of the sidelobe level. The edge excitation amplitude decreases with increasing ε . Therefore, the amplitude difference between two elements positioned next to each other becomes larger. As the amplitude difference becomes larger, excitation amplitude errors are increased by mutual coupling and manufacturing errors.

The results shown in Fig.3 and Fig.6 offer sufficient data to summarize the relation between excitation amplitude ratio and radiation pattern null depth. For example, if L_N is suppressed to within 2dB in Fig.3, R_k is less than -21dB with $L_s = -40$ dB in Fig.6 because ϵ is larger than 0.1. However if $L_N = 10$ dB is permitted, $\epsilon \approx 0.03$ and R_k increases to -15dB. Thus, the excitation amplitude taper R_k in $\epsilon = 0.03$ becomes 6dB smaller than that in the $\epsilon = 0.1$. L_N decreases with increasing ϵ , as shown in Fig.3, and R_k also decreases with increasing ϵ , as shown in Fig.6. Consequently, edge excitation amplitude is monotonously decreased with decreasing pattern null depth.

CONCLUSION

The relation between radiation pattern null depth and the resultant excitation amplitude taper was clarified. Simple formulas for null depth and amplitude taper were derived. Edge excitation amplitude was found to monotonously decrease with decreasing pattern null depth. As an example, in order to suppress null depth to within 2 dB, an amplitude taper of more than 21 dB is needed in a 20-element array. The excitation amplitude taper with 10dB-null-depth becomes 6dB smaller than that in 2dB-null depth.

ACKNOWLEDGEMENTS

The authors would like to thank Dr. Masaaki Shinji and Dr. Kenichi Kagoshima of Radio Communication Systems Laboratories, NTT, for their encouragement.

REFERENCES

- [1] Y. Yamada, Y. Ebine and N. Nakajima, "Base station / Vehicular Antenna Design Techniques Employed in High-Capacity Land Mobile Communications System", Review of ECL, Vol.35, No.2, 1987
- [2] H.J. Orchard and R.S. Elliot, "Optimising the Synthesis of Shaped Beam Antenna Pattern", IEE Proc., Vol 132, pp.63-68, February 1985
- [3] R.F. Hyneman and R.M. Johnson, "A Technique for the Synthesis of Shaped-beam Radiation Pattern with Approximately Equal-Percentage Ripple", IEEE Trans., AP-15, No.6, pp.736-743, November 1967
- [4] R.S. Elliot and G.J. Stern, "New Technique for Shaped Beam Synthesis of Equispaced Arrays", IEEE Trans., AP-32, No.10, pp1129-1133, October 1984

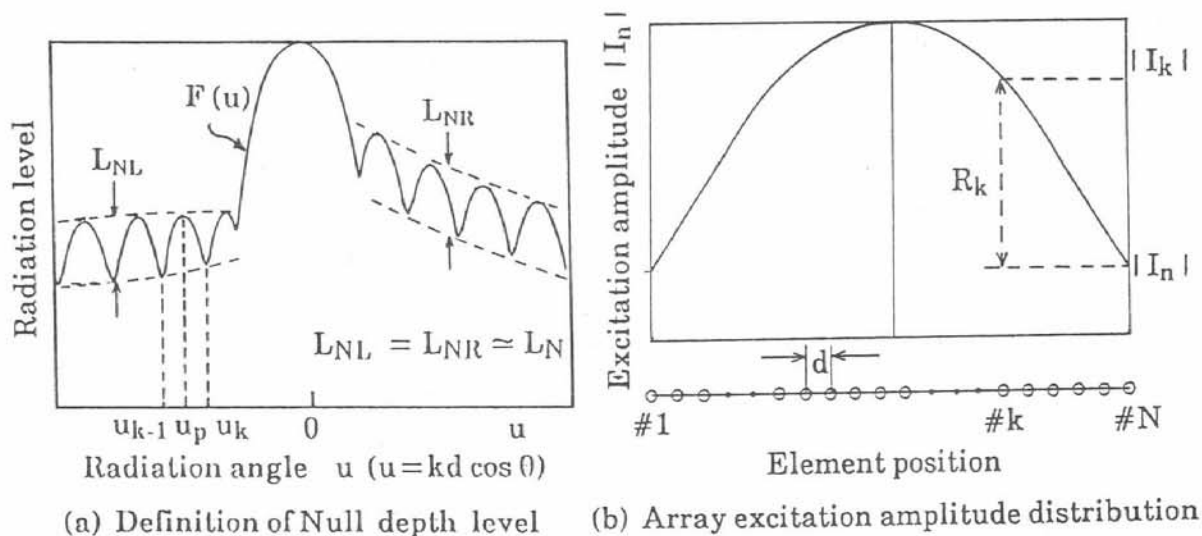


Fig. 1 Pattern nulls and excitation coefficients

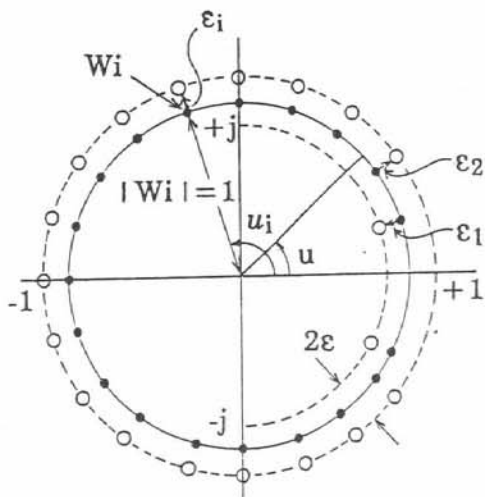


Fig. 2 Roots on and off the Schelkunoff circle

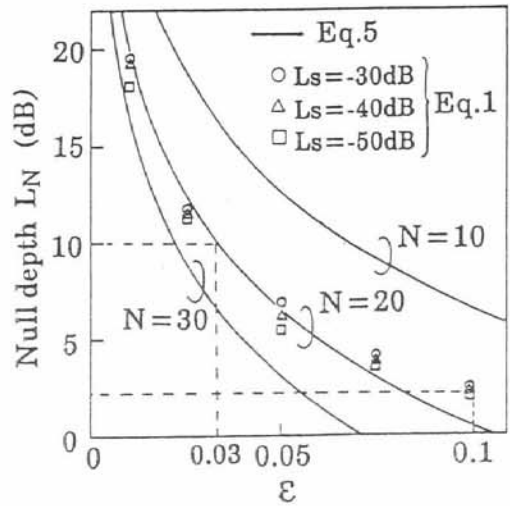


Fig. 3 Null depth dependence on ϵ

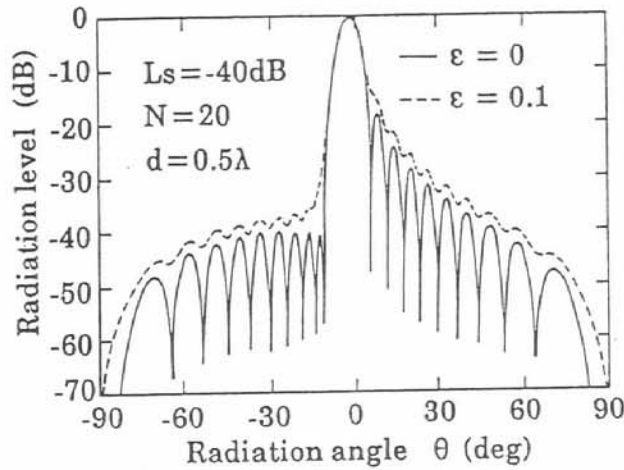


Fig. 4 Filled null radiation pattern

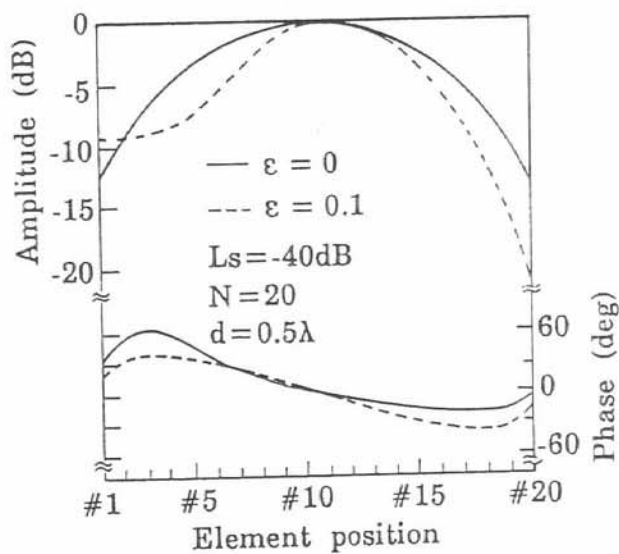


Fig. 5 Excitation coefficient of filled null pattern

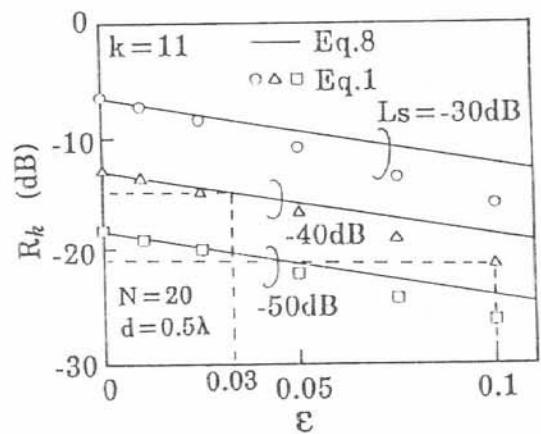


Fig. 6 Excitation amplitude ratio (R_k) dependence on ϵ